Seismic velocity estimation from well log data with genetic algorithms and comparison with neural networks and multilinear approaches

Mattia Aleardi

Link to published version: http://dx.doi.org/10.1016/j.jappgeo.2015.03.021

Abstract

Predicting missing logs is an essential tool for geophysicists. In fact, geophysical measurements in bore-holes are frequently affected by gaps in the recording of one or more logs, or else, the recording of certain logs may be performed along limited depth extensions. In particular the sonic and shear sonic logs are often recorded in limited depth extension along the well path, but their knowledge is of crucial importance for many geophysical applications. It is therefore of interest to be able to estimate the missing log intervals from a certain set of recorded logs. In this work I propose to estimate the missing part of velocity logs by making use of a Genetic Algorithm (GA) optimization and I demonstrate that this method is capable of extracting the linear or exponential relations linking the sought parameter to the other available logs. This technique has been tested on different sets of logs (gamma ray, resistivity, density, neutron, sonic and shear sonic) from three wells drilled in different geological contexts and through different lithologies (sedimentary and intrusive). The effectiveness of this methodology is demonstrated by a series of blind tests and evaluating the correlation coefficient between the true versus the predicted velocity values. Moreover, the combination of the GA optimization with a Gibbs Sampler (GS) and a subsequent Monte Carlo simulation allow us to reliably quantify the uncertainties in the final predicted velocity. In the final part the GA method is also compared with the Neural Networks approach and the

classical multilinear regression. From the comparison emerges that the GA, the NN and the multilinear methods return velocity estimations with the same prediction capability, when the relations among the input logs and the seismic velocity are close to be linear. Obviously the GA and NN approaches are more robust when the sought relations are non linear. However, in all cases, the main advantages of the GA optimization procedure, compared with the NN approach, is that it directly provides an interpretable and simple equation that relates the input and the predicted logs. Moreover, the GA method respect to the NN approach is not affected by the disadvantages that characterized the gradient descent techniques.

1. Introduction

The determination of a reliable velocity-depth trend in a particular well location is crucial in exploration geophysics. For example a reliable compressional velocity estimation is needed to perform well to seismic tie (Herron, 2014) or to derive a low frequency trend for estimating the absolute acoustic impedance from inverted post-stacked data (Morozov and Ma, 2009). Velocity logs are needed to perform an efficient AVA modeling (Mazzotti, 1991; Aleardi and Mazzotti, 2014) or to calibrate the PP and PS wave reflections (Stewart et al., 2002; Gaiser and Van Dok, 2005; Zhang and Wang, 2009). Finally, P-, S-wave velocities are of crucial importance in building rock-physics template for facies and lithology classification (Avseth et al, 2005; Dvorkin et al., 2014). However, the sonic and shear sonic logs are often recorded in limited depth extension along the well path due to the limited budget in acquiring such logs. Therefore, it is of crucial importance a reliable estimation of P-wave and S-wave velocities in the missing log interval.

This task can be accomplished by finding a specific relation which links the velocity logs with a set of other recorded logs (gamma ray, resistivity, density logs). Once these relations are known, they can be used to predict seismic velocities for the depth intervals in which data are missing or, assuming negligible lateral variations in petrophysical properties, they can be applied to predict seismic velocities to nearby wells. However, the non-linearity in the relations linking seismic

velocities to the other log data may often render their explicit evaluation a difficult task. Usually to address this drawback a linear relation between seismic velocities and the other rock properties is assumed (Pickett, 1963; Han, 1986; Castagna et al. 1993; Mazzotti and Zamboni, 2003) but this assumption is frequently violated in real cases. For examples it is well known the non linear relation linking P-wave velocity and water saturation or P-wave velocity and clay content (Avseth et al., 2005).

However, in the last few years, the development of so-called computer-based intelligence methods has enabled researchers to handle the non-linearity that characterize these optimization problems with high accuracy. In particular the artificial neural network (NN) method has received the most attention in exploration geophysics. In general, neural network technology help us in finding nontrivial correlations between geophysical data. This method has been widely applied in many geophysical problems: wavelet estimations (Wang and Mendel, 1992), velocity analysis (Calderón-Mac et al, 1998), automatic horizon picking (Huang, 1997), seismic facies classification (Coleou et al. 2003; Herrera 2006; Marroquín et al. 2008), or to relate seismic derived attributes to reservoir properties (i.e relate seismic attributes with porosity log as shown in Dorrington and Link, 2004). The NN method has been widely applied also for predicting the missing log intervals, namely to find a specific relation linking a set of input logs with another, desired log, (Arandia et al., 2001; Poulton, 2002; Srisutthiyakorn, 2012). However, notwithstanding their many successful applications in exploration geophysics the classical Neural Network approach suffers of many limitations and drawbacks. In particular, as discussed in Saggaf et al (2003) or Van der Baan and Jutten (2000), the NN method is primarily limited by its gradient-based nature.

In this study I try to overcome the drawbacks and imitations of a NN by applying a different method, namely the Genetic Algorithm, to find the linking relation between a set of input log and a desired log. In particular I focus the attention on P- and S-wave velocity predictions from a set of input log. Similarly to the classical NN approach the proposed methodology is based on the fact that seismic velocities are related to the rock petrophysical properties such as texture, mineralogy,

saturation and pore fluid content. However, other logs are also dependent on these petrophysical properties and thus, without requiring any a priori information, the GA can retrieve the existing quantitative relations among the recorded logs. Therefore, linear and/or exponential relations are assumed to relate the seismic velocities with a set of input logs and the coefficients which characterize these relations are determined performing a GA optimization.

However, the aim of any inversion or optimization process should be not only to find an optimal solution but also to quantify the uncertainties which affect the final result (Sen and Stoffa, 2013). In fact, it is know that the geophysical inverse problem suffers from the non-uniqueness problem, that is many solutions fit the observed data equally well (Tarantola, 2005). To address this problem the geophysical inverse problem is often cast in a statistical framework (Dujindam, 1988). In this statistical approach the solution of an inverse problem is not only a single set of predicted model parameters but is also represented by a posterior probability density function in model space. However, it is known that the GA (similarly to other global search algorithms) are not a Markov Chain Monte Carlo method and do not honor the principle of importance sampling (Rubinstein and Kroese, 2011). Therefore, a biased posterior probability distribution will be estimated if it is directly computed from the set of GA sampled models and their associated likelihoods (Sen and Stoffa, 1996). In particular it has been shown that the GA method is prone to underestimate the variance and thus the uncertainty associated with each inverted parameter (Sen and Stoffa, 1996; Aleardi and Mazzotti, 2014). As discussed in Sen and Stoffa (1996) MCMC methods, due to their high computational cost, can be only applied in case of a limited number of unknowns (no more than four or five). Therefore, several methods have been introduced to obtain a reliable and unbiased estimation of the posterior distributions after a GA inversion (see for example Sen and Stoffa, 1996; Mallick 1999; Hong and Sen, 2009). In this work we follow the strategy proposed by Sambridge (1999) in which a stochastic global search algorithm is combined with a subsequent resampling of the explored portion of the model space performed by a MCMC method such as the Gibbs Sampler (Geman and Geman, 1984). Therefore, this approach try to combine the speed of GA, in finding an

optimal solution, with the accuracy of a subsequent GS, to obtain a reliable estimation of the marginal probability distributions. Once that the uncertainties in the coefficient contained in the
105 estimated relation have been derived, such uncertainties are then propagated in the predicted seismic velocity via a Monte Carlo simulation (see Avseth et al 2005 for many examples of Monte Carlo simulations is exploration geophysics).

108 This paper starts with a brief overview of the genetic algorithms and of the neural network and multilinear methods. Then, I introduce the methodology that has been used to estimate the uncertainties in the regression coefficients that relate the velocity with the set of input variables.
111 After the theoretical background three different example are detailed discussed. In the final part the GA results are also compared with the NN and the classical multilinear regression.

114 **2. A brief introduction to Genetic Algorithms**

Genetic Algorithms are search algorithms developed by Holland (1975) belonging to the larger class of evolutionary algorithms, and are based on the mechanics of natural selection and evolution
117 (the "survival of the fittest" Darwinian principle) to search through model space for optimal solutions. The optimization process is driven by three main genetic operators that are mutation, cross-over and selection. In a genetic algorithm, a population of strings (called chromosomes),
120 which encodes candidate solutions (called individuals, or phenotypes) to an optimization problem, is evolved toward better solutions during the evolution process which starts from a population of randomly generated individuals. In each generation the fitness (the goodness of each possible
123 solution) of every individual is evaluated, then multiple individuals are stochastically selected from the current population on the basis of their fitness. Then they are modified (using crossover and mutation operators) to form a new population which is used in the next iteration. The algorithm
126 terminates when either a maximum number of generations has been produced, or a satisfactory fitness level has been reached for the current population. In all the following tests I set the number of individuals in the initial population to ten times the number of unknown, whereas the maximum

number of iterations is 50. In each iteration the 90% of parents is selected for reproduction and mutation. The mutation rate (the probability of mutating a variable) is fixed to 10% whereas the Stochastic Universal Sampling selection method and a linear ranking are used for selection. For replacing the parents with the generated offspring I have applied a fitness-based elitist reinsertion methods. More information and more details about GA can be found in Goldberg (1989) and Mitchell (1996).

3. The proposed methodology

Shear and compressional wave velocities depend on reservoir properties, such as the depth (z), pore fluid type (fl), lithology (lit), porosity (φ), density (ρ), and other parameters, as expressed in the following equation:

$$velocity = f(z, fl, lit, \phi, \rho .....) \quad (1)$$

Well logs inherently contain information about the reservoir properties described in equation 1 (e.g., gamma ray and resistivity logs provide lithological and pore fluid type information, respectively) and thus they can be used to estimate the P- or S-wave velocity. Moreover, if we assume that the S- or P-wave velocities are related to each log by a linear or exponential relation, equation 1 can be simply re-written as

$$velocity = \sum_{n=1}^{k} a_n input_n^{b_n} \quad (2)$$

Where the *input* variable represents the n^{th}-log used in the prediction procedure. The weight of each input variable is given by the coefficient a, whereas the exponent b aims to reproduce the effects of variations in the input log on seismic velocity.

Using a GA approach, each chromosome contains the coefficients (a_1, a_2,...,a_n,b_1, b_2,...,b_n), which express the relations between the set of input logs and the recorded velocity. The fitness of each individual is inversely correlated with the following error function:

$$error = \sqrt{\sum (d_{pre} - d_{obs})^2} \quad (3)$$

where d_{pre} and d_{obs} are the predicted and the observed velocities, respectively.

After the GA inversion the Sambridge's method (Sambridge, 1999) can be applied for attaining a reliable estimation of the marginal probability distribution for each model parameter. This method builds Voronoi cells around each sampled model, assigning the same likelihood to all points inside the same Voronoi cell. This first step creates an approximate marginal posterior probability density function (PPD) for the GA solution, then the marginal probability density functions are refined running a fast Gibbs Sampler on the approximate PPD. Therefore, in this step the portion of the entire model space explored in the previous GA optimization is resampled with a MCMC method. However, one should be careful with the initial GA set, because any error due to an insufficient sampling in GA section cannot be compensated by increasing the GS sample size. A description of the mathematical details of this method can be found in Sambridge (1999) together with practical recipes for application and how to check the final results. Applications of this approach in exploration geophysics can be found in Fliedner et al (2012) or Aleardi and Mazzotti (2014).

After the GS step we can numerically derive the marginal distribution of each coefficients (the a and b terms in equation 2). Since equation 2 is non linear the uncertainties in the final velocity distribution can not be competed analytically. Then, the marginal distribution derived from the GS resampling serve us to compute the cumulative distribution which are used to perform a Monte Carlo simulation of the final velocity distribution. This simulation is performed through 10000 Monte Carlo samples.

5. The neural network and multilinear approaches

A neural network is a mathematical algorithm inspired by the animal's central nervous system that can be trained to solve a problem that would normally require human intervention (Haykin, 1999). In particular a supervised neural network corresponds to a problem where a set of input data and their corresponding output are available: in this way, the networks can attempt to infer a relationship between the training set and the output.

Among the many different types of supervised neural networks implementations the one that has found the most applications in solving geophysical problems is the multilayer feedforward neural network (Van der Baan and Jutten, 2000). The architecture of this network mainly consists of one input layer, one output layer, and one or more hidden layers. The nodes of each layer are connected with weights, and the nodes of the hidden layers consist of non-linear or linear activation functions. The most commonly used activation or transfer function is the sigmoid function, which is a continuously differentiable, monotonically increasing function that can best be described as a smooth step function. No unique rule exists for determining the best configuration for the network structure (i.e. number of hidden layers, number of input nodes, type of activation function, number of node for each hidden layers). For more insight into this topic see Huang and Huang (1991).

Usually the NN training is performed by first setting the value of the weights to small random numbers and then updating these values using a technique called back-propagation (Haykin, 1999). This method is essentially a steepest descent algorithm. Hence it suffers from all disadvantages of the gradient-based methods. For instance, in the case of multiminima objective function, the gradient will not always point to the desired global minimum and the algorithm is prone to get trapped in local minima. To overcome this problem several authors have suggested to incorporate global search algorithms (such as Simulating annealing or Genetic algorithms) with the NN methods (for a review of such methods see Van der Baan and Jutten, 2000). These hybrid methods are not considered here.

Following, Mazzotti and Zamboni (2003) a stepwise regression (Draper and Smith, 1985) will be applied in the multilinear approach. Basically this method is a semi-automated process of deriving a linear equation by successively adding or removing variables in the regression procedure basing solely on the t-statistics of their estimated coefficients. There are three main approach to this regression method: Forward selection, backward elimination and bidirectional elimination. The first starts with no variable in the model and proceed forward (adding one variable at a time). The second start with all potential variables in the model and proceed backward (removing one variable

at a time). In this work we applied the third method which is a combination of the above mentioned approaches. This is essentially a forward selection procedure but with the possibility of eliminating a selected variable at each optimization stage.

4.1 Example 1: Estimating Vs in a shale-sand sequence

In the first case, I compute the S-wave velocity from the variables depth (Z), gamma ray radiation (GR), density (DEN) and deep resistivity (RES). The relations between S-wave velocity and each input log are shown in the cross-plots of Figure 1.

The used logged interval spans from 3700 m to 4000 m below sea level (Figure 1a), and due to this limited depth range, the depth variable shows a weak influence on the S-wave velocity. Figures 1b and d show that the density and the gamma ray radiation versus the shear wave velocity separate into two classes: the shales, with high densities and high gamma ray radiation, and the sands, with significantly lower values for both indicators. A strong interdependence between the S-wave velocity and resistivity is evident in the cross-plot of Figure 1c, where the samples in the upper right corner pertain to gas-saturated sands.

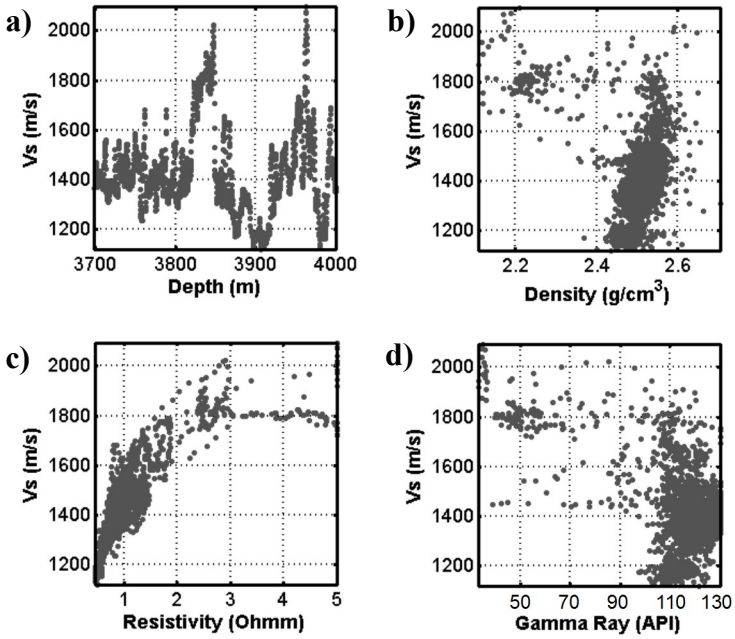

Figure 1: Cross-plots of the measured S-wave velocities against each input log used in the optimization procedure .a) S-wave velocity vs. depth. b) S-wave velocity vs. density. c) S-wave velocity vs. resistivity. d) S-wave velocity vs. gamma ray radiation.

Using the GA to find the relations among the input logs and the S-wave velocity (as indicated in

219 equation 2), for this example, I find the following expression:

$$Vs_s = 0.27\, Z_s^{0.99} + 0.43\, DEN_s^{2.94} + 0.3\, RES_s^{0.68} + 0.01\, GR_s^{-0.45} \quad (4)$$

In equation 4, to better compare the values assumed by each coefficient, I have scaled the log data to a mean of one (as indicated by the subscript *s*). Figure 2 shows the Vs velocity computes

222 according to equation 4. Velocity is plotted versus depth and density (Figure 2a) and versus resistivity and gamma ray (Figure 2b).

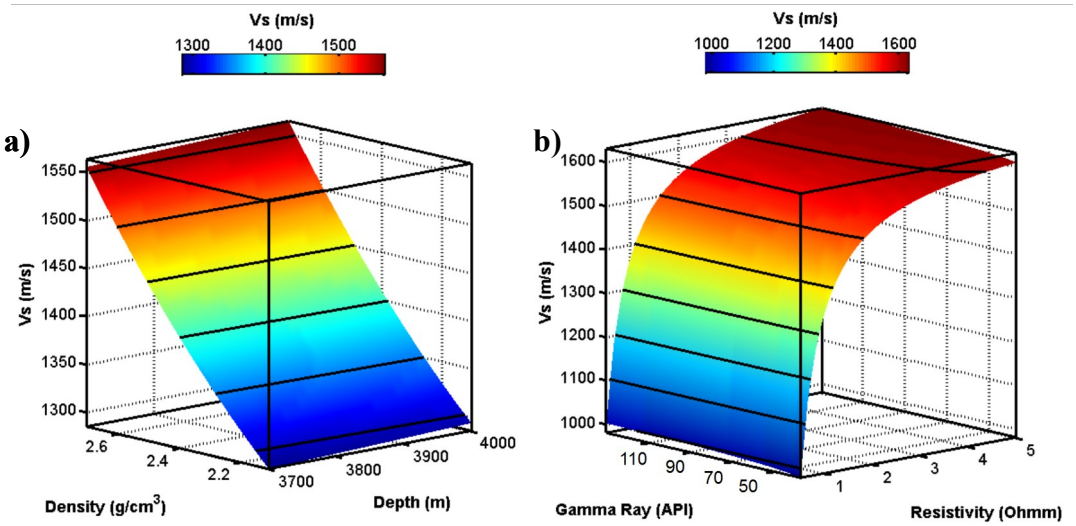

Figure 2: Graphical representation of the terms in equation 4: the relations linking each input log with the S-wave velocity as estimated by the GA optimization. a) influence of Depth and Density on Vs. b) influence of Gamma Ray and resistivity on Vs. Note the strongly non-linear relation between Vs and resistivity. The black lines indicate the velocity isolines.

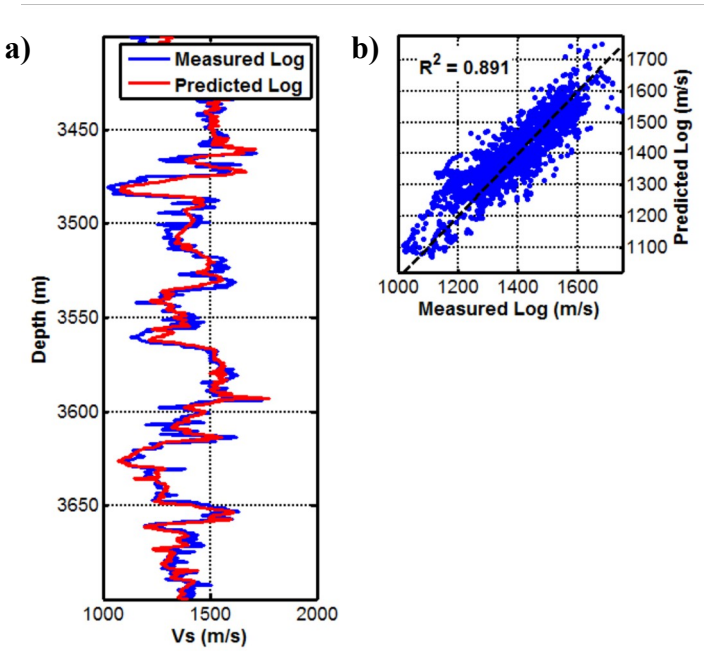

Figure 3: a) Comparison between the real and the predicted velocity versus depth. b) Cross-plot between the real and the predicted velocity with the resulting correlation coefficient R^2.

225 Figure 2 shows that the most important variables in this regression are density and resistivity, whereas the gamma ray information has a minor effect on the S-wave velocity estimation. The quantitative relations of equation 4 have been derived by considering short segments of the logged 228 intervals for which all of the logs, including the velocity logs, are available. Therefore, to verify the applicability of equation 4 in predicting the velocity, I have performed a blind test outside the used log interval. The result of the blind test for this example is illustrated in Figure 3. Figure 3a shows a 231 close-up of the real, that is the logged, velocity (blue curve) and the predicted velocity (red curve). Note the satisfactory match between the two curves for this first example. Figure 3b shows the regression plot and the correlation coefficient (R^2) for the real and predicted velocities. Very high 234 correlation is achieved in this case. After the GA optimization aimed at deriving the relation shown in equation 4, the entire set of models (each one representing a different combination of the coefficients and exponent a_n and b_n of equation 2) and their associated likelihoods have been used in 237 the GS resampling. In deriving the final posterior probability we have assumed an uninformative prior model uniformly distributed in the entire search range for each inverted parameter. In this contest the final posterior probability density function is mainly influenced by the likelihood 240 function. For deriving the likelihood associated with each explored model the classical formula described in Sen and Stoffa, 1996 have been applied.

Figures 4a, b, c and d illustrate examples of the final marginal posterior distributions pertaining 243 to the coefficient and exponent of the depth and density logs. A very good resolution is attained in both cases. The final marginal distributions have been used to perform a Monte Carlo simulation in order to propagate the uncertainties in the regression coefficient to the uncertainties in the seismic 246 S-wave velocity. In this simulation each model parameters has been considered as an indipendent realization. The simulation, performed employing 10000 Monte Carlo samples, yields the final S-wave velocity distribution shown in Figure 5. Note the very high resolution obtained in this 249 example.

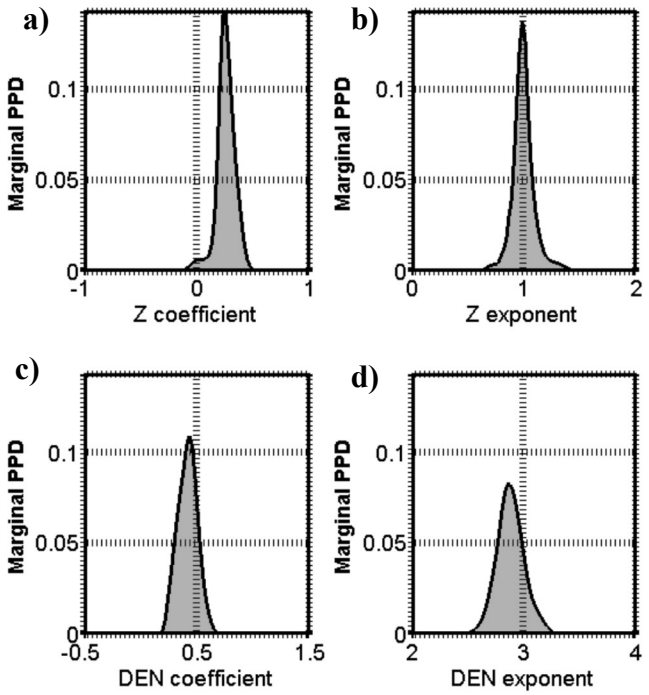

Figure 4: Examples of the final marginal distributions derived after the GS resampling. a) and b) marginal distributions for the z coefficient and z exponent, respectively. c) and d) Marginal distributions for the density coefficient and density exponent, respectively.

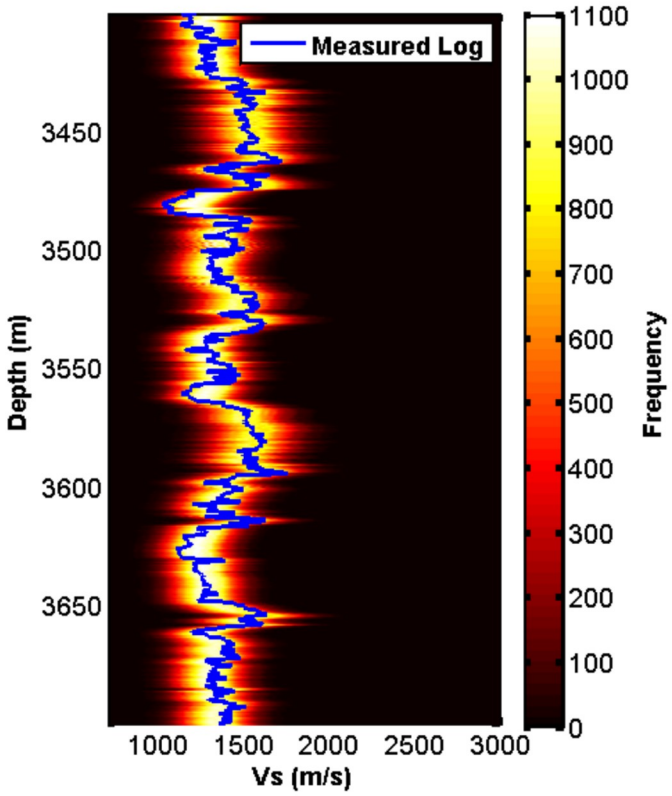

Figure 5: Predicted S-wave velocity distribution derived after the Monte Carlo simulation and using the marginal distribution of each regression coefficient of equation 4 has been obtained combining the GA optimization with the GS method.

4.2 Example 2: Estimating Vp in a shale-sand sequence

The second case differs from the previous one in that only gamma ray and density logs are
255 available in addition to the standard sonic log. Although the used depth range is limited from 200 m to 350 m below the rotary table, it is clear (Figure 6a) that the depth has a significant impact on the P-wave velocity.

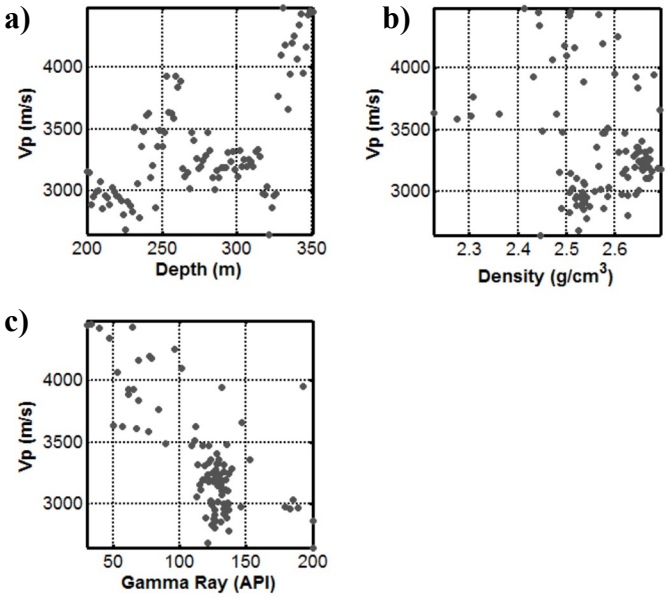

Figure 6: Cross-plots of the measured P-wave velocity against each input log used in the optimization procedure. a) P-wave velocity vs. depth. b) P-wave velocity vs. density. c) P-wave velocities vs. gamma ray radiation.

258 In Figures 6b and c, the two populations of sands and shales are distinguishable on the basis of their P-wave velocities and gamma ray radiation, with the shales having lower velocities and higher gamma ray radiation than the sands. In this second case the GA finds the following equation to
261 relate the variables depth, density and gamma ray radiation to the P-wave velocity:

$$Vp_s = 0.53\, Z_s^{0.71} + 1.16\, DEN_s^{0.07} - 0.7\, GR_s^{0.41} \quad (5)$$

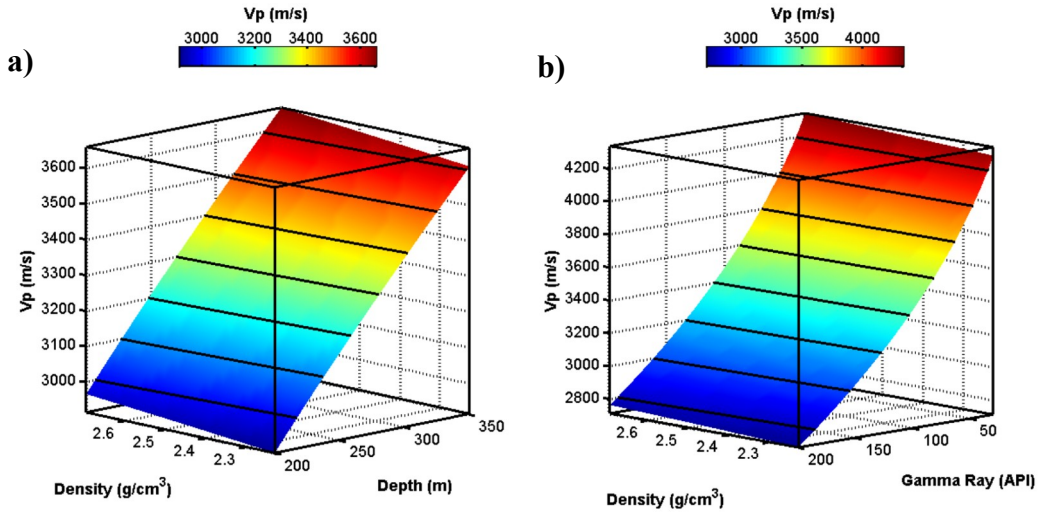

Figure 7: Graphical representation of the terms in equation 5: the relations linking each input log with the P-wave velocity as estimated by the GA optimization. a) influence of Depth and Density on Vp. b) influence of density and Gamma Ray on Vp. The black lines indicate the velocity isolines.

As in equation 4 the subscript *s* indicated the scaled version of the considered logs.

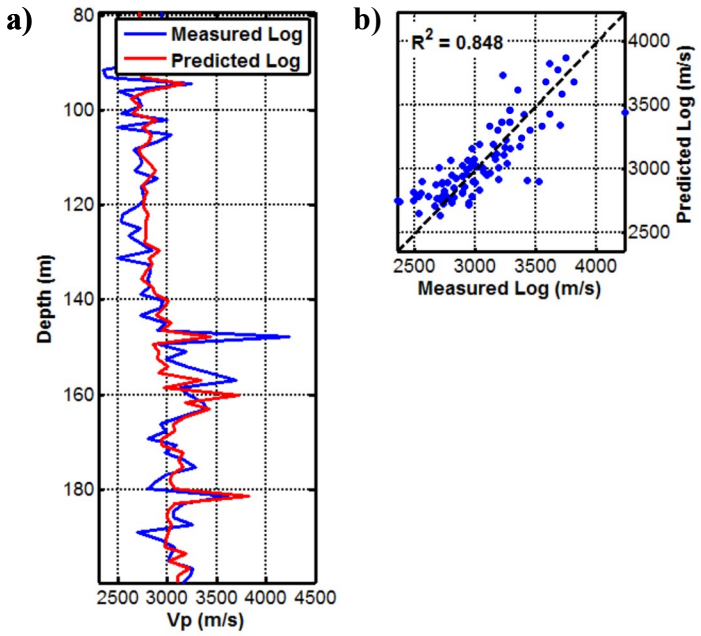

Figure 8: a) Comparison between the real and the predicted velocity versus depth. b) Cross-plot between the real and the predicted velocity with the resulting correlation coefficient R^2.

Figure 7 shows the influence of each input variable (depth, density and gamma ray) on the P-
264 wave velocity. In this case, in addition to the depth and the density variables, the gamma ray radiation exerts a major effect on the P-wave velocity. In contrast to the previous case for the S-wave velocity, the shale content strongly influences the P-wave velocity prediction. Figure 7 also
267 shows that in this case, likely due to the rather limited depth range, the relations display a quasi-

linear behavior. The result of the blind test for this example is illustrated in Figure 8, where good prediction is shown by comparing the measured and predicted velocity and by the correlation coefficient (R^2) (Figure 8a and b, respectively). Even in this example, where i have used only two input logs (density and gamma ray) and a very limited depth interval (200 m-350 m), the match is good. Furthermore, the anomalous velocity values present in the actual log (such as the high velocity peak near a depth of 150 m) can be corrected using the predicted values. Also in this case after the GA optimization the uncertainty in the final Vp has been quantified by means of the GS step, aimed at determining the uncertainties in the regression coefficient in equation 5, and of the successive Monte Carlo simulation. Figure 9 represents the final uncertainty in the P-wave velocity estimation. Also this example is characterized by a satisfactory resolution on the velocity value.

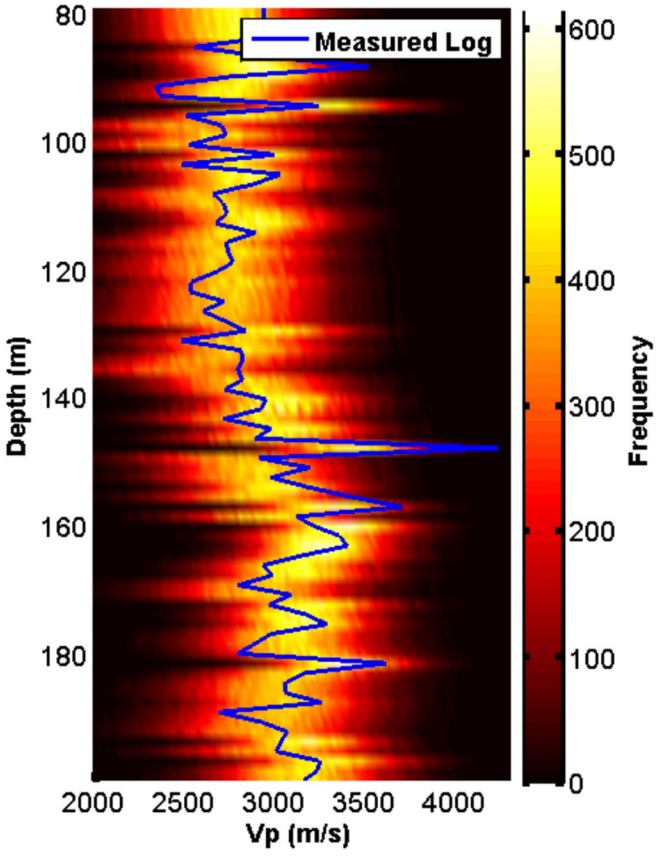

Figure 9: Predicted P-wave velocity distribution derived after the Monte Carlo simulation and using the marginal distribution of each regression coefficient of equation 5 has been obtained combining the GA optimization with the GS approach.

4.3 Example 3: Estimating Vs in a fractured intrusive rock

In contrast to the previous two cases for different sand and shale sequences, the third case considers a geothermal reservoir hosted in an intrusive fractured rock.

In this example, I attempt to estimate the S-wave velocity using the depth, P-wave velocity and resistivity information. In this case, the depth interval used in the estimation procedure ranges from 2980 to 3120 m below the rotary table. As shown in Figure 10a, it is clear that the depth has a minor influence on the S-wave velocity in this interval, which shows a clear quasi-linear correlation with the P-wave velocity and resistivity (Figures 10b and c, respectively). The increase in the S-wave velocity with resistivity can be explained by considering the low resistivity values pertaining to the fractured intervals inside the intrusive rock. In this last example, I have derived the following formula relating the S-wave velocity to the input logs:

$$Vs_s = 0.3\, Z_s^2 + 0.48\, Vp_s^{1.05} + 0.2\, RES_s^{1.8} \quad (6)$$

The predicted relations between the S-wave velocity and the input logs are illustrated in Figure 11. In this case the S-wave velocity is plotted versus depth and P-wave velocity (Figure 11 a) and versus P-wave velocity and resistivity (Figure 11 b and c). From this figure emerges the strong influence of the Vp and resistivity in determining the Vs values and the minor role played by the depth.

The results of the blind test show a lower correlation coefficient (Figure 12b) than in the previous cases, most likely due to the more complex geological context and the lower performance of the logging tools in these lithologies at high temperatures. However, Figure 12a, presenting a comparison between the real and predicted S-wave velocity values, shows that the results of the blind test are satisfactory. In particular, we can estimate the sudden decrease in S-wave velocity occurring near 3350 m due to the presence of a fractured zone. Therefore, for this more stringent test, the reliability and applicability for predicting the velocity values are confirmed.

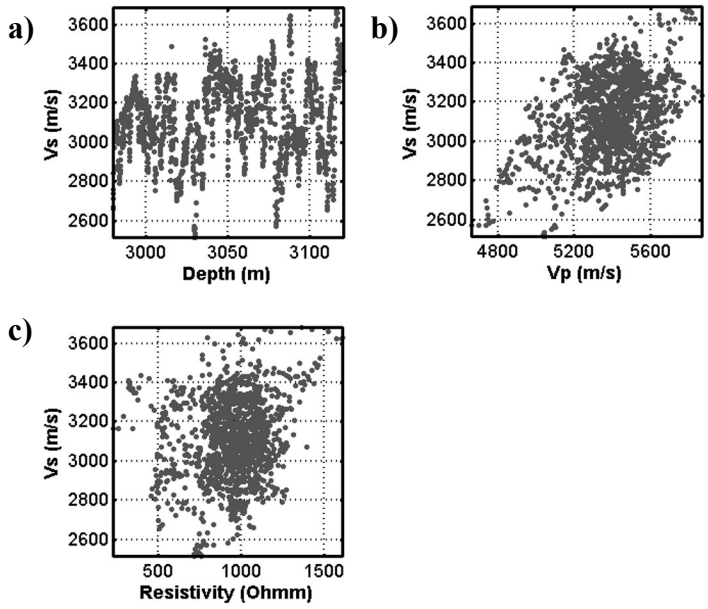

Figure 10: Cross-plots of the measured S-wave velocities against each input log used in the optimization procedure. a) S-wave velocity vs. depth. b) S-wave velocity vs. Vp. c) S-wave velocities vs. resistivity.

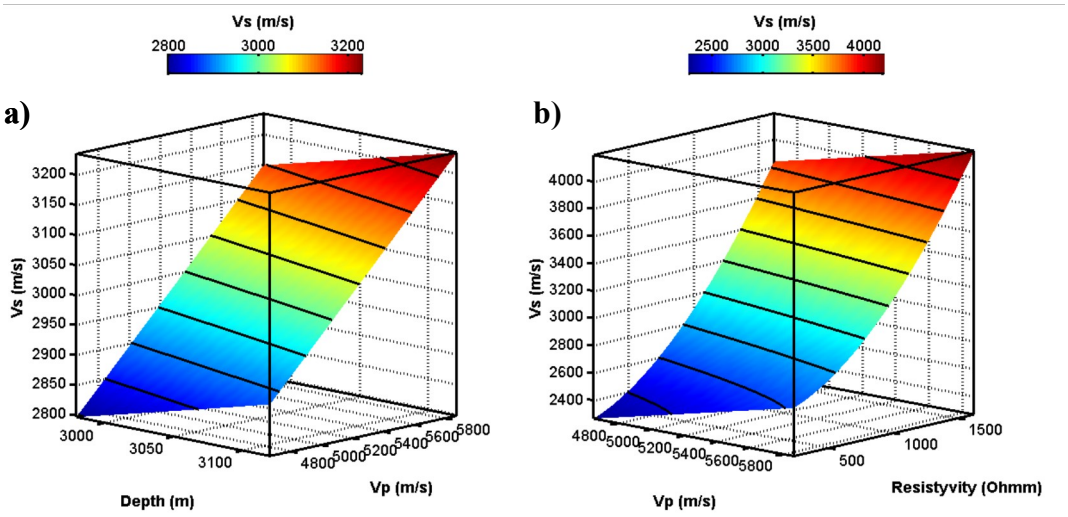

Figure 11: Graphical representation of the terms in equation 6: the relations linking each input log with the S-wave velocity as estimated by the GA optimization. a) influence of Depth and P-wave velocity on Vs. b) influence of P-wave velocity and resistivity on Vs. The black lines indicate the velocity isolines.

303 Similarly to the previous example, the GA optimization has been followed by the GS step to reliably determined the uncertainties in the regression coefficient shown in equation 6. Examples of the final marginal distributions pertaining to the coefficient and exponent associated with the 306 resistivity variable are illustrated in Figure 13. In this case due to the very complex geological contest and to larger scatter visible in Figure 10 the marginal distribution are multimodal. In addition, if we compare Figure 13 with Figure 4 (showing examples of the marginal distribution in

the first example) we can appreciate the larger uncertainty (larger variance) which characterizes this third example. These ambiguities reflects on the uncertainties in the final S-wave velocity prediction derived after the successive Monte Carlo simulation (Figure 14). In Figure 14 is clearly evident the larger ambiguities in the seismic velocity prediction in this example with respect to the previous two (compare Figure 14 with Figures 5 and 9). However, the overall velocity-depth trend is recovered also in this example.

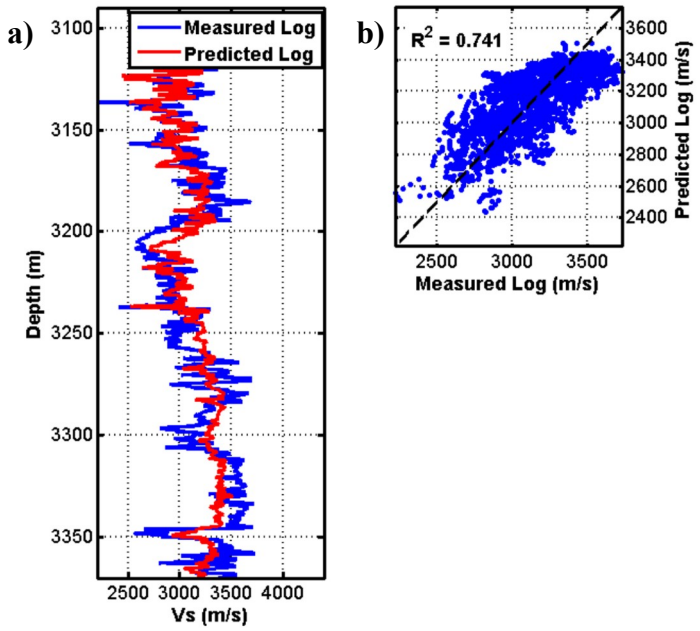

Figure 12: a) Comparison between the real and the predicted velocity versus depth. b) Cross-plot between the real and the predicted velocity with the resulting correlation coefficient R^2. Notwithstanding the lower regression coefficient attained in this example compared to the previous ones, the derived equations are able to predict the sudden decrease of S-wave velocity around 3350m due to a fractured zone in the igneous rock.

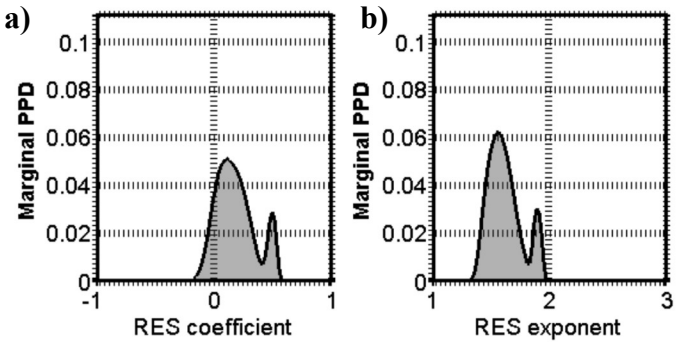

Figure 13: Examples of the final marginal distributions derived after the GS step. a) and b) marginal distributions for the resistivity coefficient and exponent, respectively. Note the multimodality of the distribution and also the larger variance compared to the probability distributions shown in Figure 4 (the x-axis scale is the same in both figures).

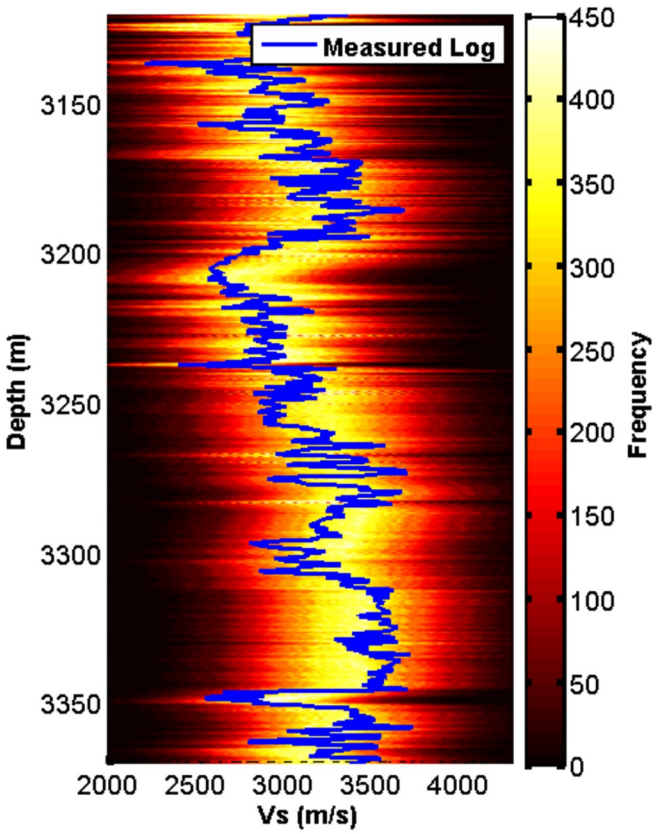

Figure 14: Predicted S-wave velocity distribution derived after the Monte Carlo simulation and using the marginal distribution of each regression coefficient of equation 6 has been obtained combining the GA optimization with the GS sampling. Note the larger uncertainties with respect to the first and second examples (Figures 5 and 9). For a better comparison the x-axis scale is the same in all these figures.

5.1 Comparison between GA, NN and multilinear inversion.

In this chapter I compare the outcomes of the GA optimization procedure with those obtained with the very popular NN approach and the classical multilinear stepwise regression. Also for the NN and the stepwise inversion optimization I perform a series of three blind tests considering the same depth intervals used in the previous GA examples in the prediction procedure and for extending the derived relations.

For what concerns the NN architecture in the following examples, I have used one hidden layer with 16 neurons with a sigmoid transfer function. The input layers have as many nodes as input logs, and the weights are computed such that the value at the output layer is equal to the training

value in the least-squares sense. Finally, the early stopping criterion is applied to stop the NN optimization and to prevent overfitting the training samples (Van der Baan and Jutten, 2000).

Figures 15a shows the comparison between the GA, NN and multilinear results for the first example regarding the Vs estimation in the shale-sand sequence. In this case very similar results are attained by the GA and NN method while it is interesting to observe that the multilinear approach return less accurate results as shown by the percentage error represented in Figure 15b. This is likely do to the strongly non linear relation that exists, in this case, between Vs and resistivity (see equation 4 and Figure 2b) that the multilinear regression can not predict.

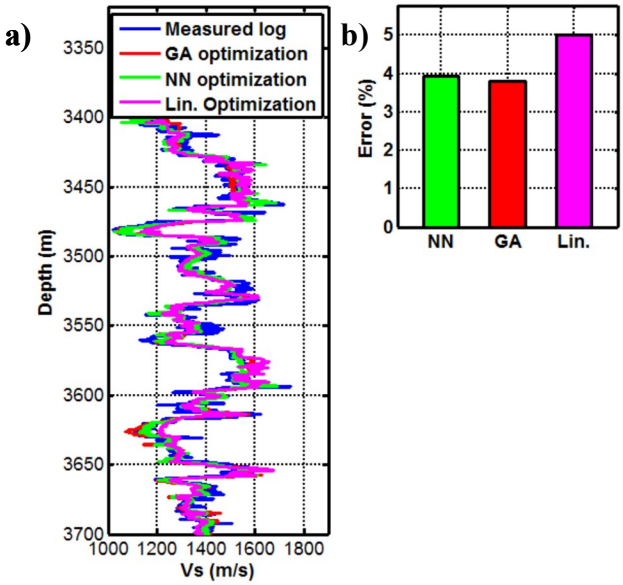

Figure 15: a) Comparison between the true, recorded Vs velocity and the predicted velocities by the GA, NN and multilinear (Lin.) optimization techniques for the shale-sand sequence considered in the first example. b) the percentage error pertaining to each method.

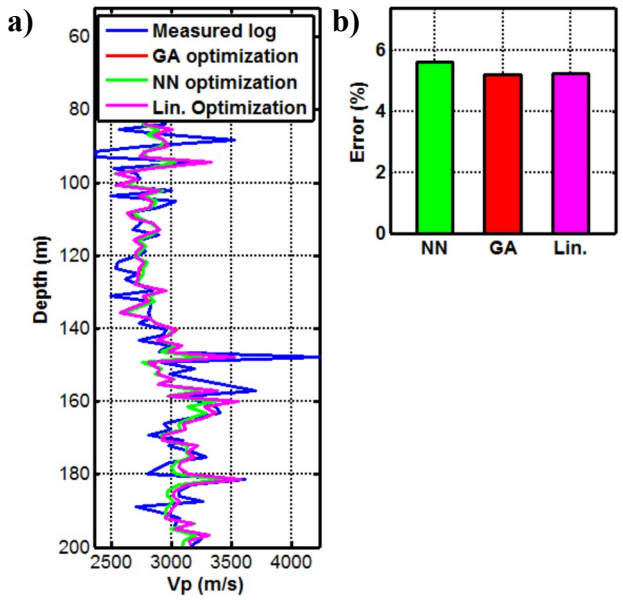

Figure 16: a) Comparison between the true, recorded Vp velocity and the predicted velocities by the GA, NN and multilinear (Lin.) optimization techniques for the shale-sand sequence considered in the second example. b) the percentage error pertaining to each method.

336 Figure 16a and b illustrate the comparison between the recorded P-wave velocity and the predicted ones by the GA, NN and multilinear optimizations and the final percentage error, respectively. Being the relations between the Vp and the other input variables very close to be linear 339 the three methodologies return very similar results.

Figure 17a and b illustrate the comparison between the three methods for the third example. Also in this case the comparison shows very similar results.

342 However, as previously seen in Figure 15 a non linear method (such as the NN or the GA approach) can be more accurate, respect to the classical multilinear regression, in case where a clearly non linear relation exist between an input variable and the desired log.

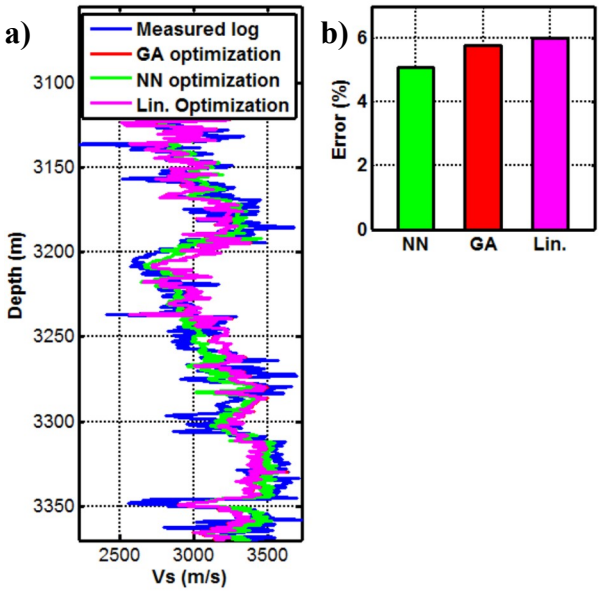

Figure 17: a) Comparison between the true, recorded Vs velocity and the predicted velocities by the GA, NN and multilinear (Lin.) optimization techniques for the third example. b) the percentage error pertaining to each method.

345 However, among the non linear methods, the main advantage in utilizing the GA optimization respect to the NN method, is that this approach directly provides an interpretable and simple equation relating the input and the predicted logs. In addiction the NN method is essentially a linear 348 gradient-based optimization and then, it is not well-suited for uncertainties analysis because only a very small and localized model space portion is explored during the inversion. Differently the GA method is able to explore different model space zones and thus the entire set of explored models 351 and associated likelihoods can be used to quantify the uncertainties affecting the coefficients in the derived equation. However, I remind that the GA method is not a MCMC algorithm and then for attaining an unbiased estimation of the marginal probability of each inverted parameter, I have 354 combined the stochastic optimization with the following GS method. A last remark must be made for what concerns the differences between the classical NN and the GA methods. Usually in a NN optimization the weights associate to each neuron are randomly initialized and are subsequently 357 optimized by means of a gradient-based strategy. This make clear the importance of a good starting model to prevent the convergence toward a local minimum in case of complex multiminima misfit function. To overcame these limitations the NN optimization must be repeated many times, starting 360 from different starting models, from which the best result will be selected. This procedure can be very time consuming in case of a huge numbers of training samples. An alternative procedure, not

discussed here but mentioned by several authors (for a review see Van deer Ban and Jutten, 2000), is to use a global training scheme to obtain several good initial guesses to start a localized inversion. However, the GA method, or other global search algorithms, circumvent this drawback by performing in a single inversion run a wide and efficient exploration of the entire model space. In this way the final result is much less affected by multiple minima and by the initial guess of the starting model.

6. Conclusions

The good match between the measured and predicted seismic velocities demonstrates the potential of genetic algorithms to yield prediction equations capable of estimating the shear and compressional wave velocities from a set of input log data to a good degree of approximation. A slightly lower correlation and matching were observed for the intrusive rock example. This result might be due to the more complex geological context and the lower performance of the logging tools in the lithologies at high temperatures.

Moreover, these examples demonstrate the relations linking seismic velocity with the other logs exhibit a strongly case-dependent behavior, that is, the a and b coefficients of equation 2 for the same log can be quite different from case to case.

If needed, the predicted relations can be extended along the well path, where velocity measures have not been measured or are affected by errors, or, assuming negligible lateral variations, to nearby wells. This same approach has also been applied to the prediction of other quantities, such as the porosity, density or resistivity, from a set of input logs that may include P- and S-wave velocity measures, and also in these cases, high-quality results were obtained.

Combining the GA algorithm with a Markov Chain Monte Carlo method, such as the Gibbs Sampler, enables us to quantify the uncertainties in the derived equations. Through a resampling of the model space explored during the GA optimization it is possible to derive an unbiased estimation of the posterior marginal probability distribution associated to each coefficient in the final equation.

Comparing the results produced by the GA approach with the outcomes derived from a neural network method and a multilinear inversion it turns out that the three methods give rise to very similar results when the relation between velocity and the set of input logs is linear. When the relations are strongly not linear it is advisable to apply a non linear optimization such GA or NN method. However, the main advantage of the GA optimization procedure respect to the NN, is that it directly provides an interpretable and simple equation relating the input and the predicted logs. Moreover, the GA method overcomes the well known limitations (i.e entrapment in local minima, results strongly dependent on the initial guess of the starting model) that frequently affect the NN approach. Finally, the GA method is best suited respect to the NN, in casting the inversion problem in a probabilistic framework. In fact after the GA inversion the entire set of explored models and associated likelihood can be used to quantify the uncertainties affecting the final result.